REPORT DOCUMENTATION PAGE

Form Approved OMB No. 0704-0188

1. REPORT DATE *(DD-MM-YYYY)*	2. REPORT TYPE	3. DATES COVERED *(From - To)*
	Technical Paper	

4. TITLE AND SUBTITLE	5a. CONTRACT NUMBER
	5b. GRANT NUMBER
	5c. PROGRAM ELEMENT NUMBER
6. AUTHOR(S)	5d. PROJECT NUMBER
	5e. TASK NUMBER
	5f. WORK UNIT NUMBER
7. PERFORMING ORGANIZATION NAME(S) AND ADDRESS(ES)	8. PERFORMING ORGANIZATION REPORT
9. SPONSORING / MONITORING AGENCY NAME(S) AND ADDRESS(ES) Air Force Research Laboratory (AFMC) AFRL/PRS 5 Pollux Drive Edwards AFB CA 93524-7048	10. SPONSOR/MONITOR'S ACRONYM(S) 11. SPONSOR/MONITOR'S NUMBER(S)

12. DISTRIBUTION / AVAILABILITY STATEMENT

Approved for public release; distribution unlimited.

13. SUPPLEMENTARY NOTES

14. ABSTRACT

15. SUBJECT TERMS

16. SECURITY CLASSIFICATION OF:			17. LIMITATION OF ABSTRACT	18. NUMBER OF PAGES	19a. NAME OF RESPONSIBLE PERSON
a. REPORT	b. ABSTRACT	c. THIS PAGE			Leilani Richardson
Unclassified	Unclassified	Unclassified	A		19b. TELEPHONE NUMBER *(include area code)* (661) 275-5015

3 items enclosed

TP-FY99-0161

3005001

ltr # = F04611-96-C-0023

/DTI

MEMORANDUM FOR PRR (Contractor Publication)

28 June 1999

FROM: PROI (TI) (STINFO)

SUBJECT: Authorization for Release of Technical Information, Control Number: AFRL-PR-ED-TP-FY99-0161
Hruby... (Busek), "Development of Low Power Hall Thrusters"
30th Plasmadynamics & Laser Conference **(Statement A)**

99-3534

DEVELOPMENT OF LOW POWER HALL THRUSTERS

V. Hruby, J. Monheiser, B. Pote, P. Rostler, J. Kolencik and C. Freeman
Busek Co. Inc., Natick, MA 01760-1023

Abstract

Three different types of sub kilowatt class Hall thrusters for on-board propulsion of small to mid size satellites are being developed at Busek. This paper describes their performance focusing on plasma behavior outside of the thrusters and contrasts the typical Hall thruster plasma with that encountered in MHD generators and accelerators researched in the past and familiar to the plasmadynamic community. A simple performance predicting analytical model, applicable to all sizes of thrusters also is presented. It adequately matches the measured thrust and specific impulse expressed in terms of primary electron loss parameter, and an overall voltage loss which includes the loss in the plasma bridge between the external cathode and the thruster. The external plasma plume was surveyed using a Faraday cup and an emissive probe to measure the beam current and the plasma potential. These measurements, together with the model support our visual observation that the plume, of a well performing thruster, forms at its center a highly conductive jet with sharply defined cone shaped boundaries. These boundaries were tentatively identified as an ion acoustic shock. The preliminary data and analysis indicate that the plasma downstream of the ion acoustic shock is at least partially responsible for the widely reported correlation between increasing test tank pressure and an increase in performance of Hall thrusters.

Introduction

The plasma dynamic community is familiar with the magnetohydrodynamic (MHD) generators and accelerators in development during the last several decades whose plasma is dominated by collisions. It is however less familiar with the low pressure, nearly collisionless, glow discharge encountered in the typical electrostatic and electromagnetic plasma accelerators used for space propulsion. The discussion below contrasts the two plasma regimes and the practical consequences of their differences.

A thirty year period starting in the late fifties saw an explosion in MHD research Ducted flow MHD decelerators (generators) that extracted energy from the fluid to produce power were studied most extensively.[1,2,3] The fluids were high temperature molecular or monoatomic gases seeded with alkali metals to increase their conductivity or liquid metals.[4] Devices that accelerated fluids received less attention but were researched for propulsion purposes, for fluid transfer (e.g. liquid metal pumps) and for increasing the enthalpy of gaseous streams for hypersonic wind tunnel research.[5]

Ducted accelerators that were studied included MHD rockets where some gaseous plasma was accelerated out of a nozzle to produce thrust[6,7] and the same principles were also applied to MHD ship or submarine propulsion.[8] More recently, external flows of plasma, manipulated by application of magnetic field and power were studied to control boundary layers on hypersonic vehicles and replace their solid wall control surfaces by electromagnetic interaction.[9]

All of the above cited gaseous plasmas had one feature in common. The mean free path of the plasma ion in a cloud of neutral species is small and the plasma is highly collisional. Under these circumstances the charged species and the neutrals behave as a coupled fluid and can be, without any difficulty, described by the classical Ohm's law in vector form

$$\bar{J} + \bar{\beta} \times \bar{J} = \sigma\left(\bar{E} + \bar{u} \times \bar{B}\right) + \text{diffusion term} \qquad [1]$$

where J is current density, β is Hall parameter, σ is conductivity, E is electric field, B is applied magnetic field and u is the coupled fluid velocity. The diffusion term is safely neglected in high pressure, partially ionized, collision dominated plasma of a typical MHD generator and the effective Hall parameter rarely exceeds 3[10]. When the plasma density decreases to a point where ion neutral collisions are rare, the fluid is no longer coupled, significant fraction of the total current is transported by ions, and the Hall parameter can increase to a value unattainable in collisional plasmas. The diffusion term in Eq. [1] becomes relevant and due to the high electron mobility ($\mu = \beta/B$), a Hall parameter of the order of 100 and larger can be achieved with B of the order of 100 Gauss instead of several the Tesla required by the higher pressure MHD devices referenced above. This,

---

*Principal Investigator, Member AIAA
†Research Scientist, Senior Member AIAA
‡Principal Engineer, Member AIAA
§Senior Scientists, Member AIAA
¶Engineering Aid
#Engineering Aid

combined with the low plasma collisionality has enormous practical consequences. Large, many meters long super conducting magnets are not required and the size of useful devices goes down by two orders of magnitude. One such useful device is an electromagnetic/MHD plasma accelerator that can efficiently operate with an input power as low as 50 Watts. It can be used for terrestrial applications (e.g. sputtering and ion milling) or in space propulsion. In the propulsion community it is known as the Hall thruster (or a SPT thruster in Russia where much of the development was done[11]) because it relies on the Hall parameter to create the ion accelerating electric field.

The typical Hall thruster, shown schematically in Fig. 1, is an axisymmetric device with annular dielectric cavity where the discharge occurs. The plasma gas, (preferably a heavy monoatomic gas such as Xe) is introduced at the upstream end of this cavity, frequently through the positive polarity electrode (the anode). Proceeding through the cavity, the neutrals encounter a zone with high electron density and steeply rising radial magnetic field (Br~10^{-2} Tesla). The high Br, created by permanent or electromagnets, traps electrons that originate in an external cathode, forcing them to execute the so called $\overline{E} \times \overline{B}$ drift. Due to this drift the electron azimuthal flow is 100 to 200 times larger than the axial current and hence the Hall parameter is of the same order ($\beta \sim J_z/J_\theta$). The high current density (J_θ ~10 to 100 A/cm^2) creates strong axial electric field ($E_z \approx 10^5$ V/m) and leads to high rate of collisions with neutral gas which ionizes. Ions remain largely unaffected by Br and get accelerated outward by the coulomb force (=qE_z where q is the ion charge) creating thrust. In a good thruster 90% of the flow is transported by ions. Although not a very useful paradigm, but one familiar to the MHD generator researchers, one could think of the acceleration force as the Lorentz force (~J_θBr).

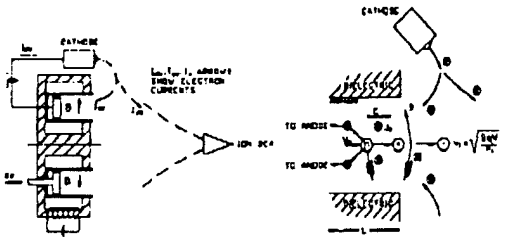

Fig 1 Cross-sectional schematic of a typical Hall thruster detailing the ionization and ion acceleration process

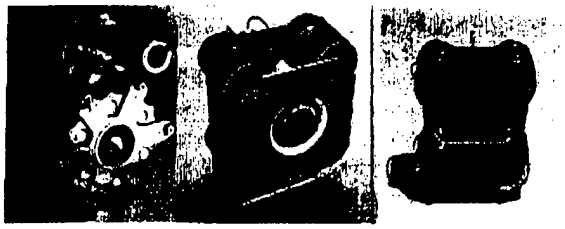

Fig 2 Low power Hall thrusters under development at Busek. Starting from left is a 200 W thruster with a cathode, 600 W thruster and 150 W racetrack thruster

Hall thrusters are rapidly becoming the propulsion of choice for many satellites and there is a large effort devoted to the development of Hall thrusters world wide.[11,12,13,14] Their popularity is due to their simplicity and performance parameters that fit most missions with a typical specific impulse (I_{sp}) of 1600 sec (Xe gas and 300 Volts discharge voltage) and typical thrust efficiency (η) of 50%.

Busek is developing, with government and private funding, several types of Hall thrusters ranging from 200 W to 8 kW. This paper will focus on the smallest devices, those in the sub-kW class that are shown in Fig. 2. Starting from the left, there is a nominally 200 W Tandem Hall thruster designated BTHT-200, a 600 W, high plasma density thruster, designated BHT-HD-600 and a non-circular, nominally 200 W racetrack shaped device designated BHT-RT-150. Although their internal design is radically different from each other, we will show that their performance and the performance of all Hall thrusters, can be described by a simple parametric model and that the plasma behavior downstream of their exit plane significantly influences their performance.

Test Facility and Test Procedures

All tests reported herein were conducted in Busek's T6 vacuum facility. This facility, shown in Fig. 3, has two liquid nitrogen (LN_2) cooled sections, one where the experimental apparatus is located and the second where the pumping is accomplished. The experiment section is 1.8-m in diameter and 1.8-m in length while the pumping section is 2.4-m in diameter and 1.2-m in length. Pumping is accomplished by a 0.8-m diameter oil diffusion pump used to pump the low molecular weight gases and four cryo-panels used to pump xenon. In full operation (i.e. diffusion pump plus cryo-panels) the facility is capable of pumping 90,000 l/sec of xenon and with only the diffusion pump operating, the facility pumps ~8,000 l/sec of xenon. An LN_2 baffle, located above the diffusion pump is used to prevent any hot oil vapor from reaching the experimental section of the facility.

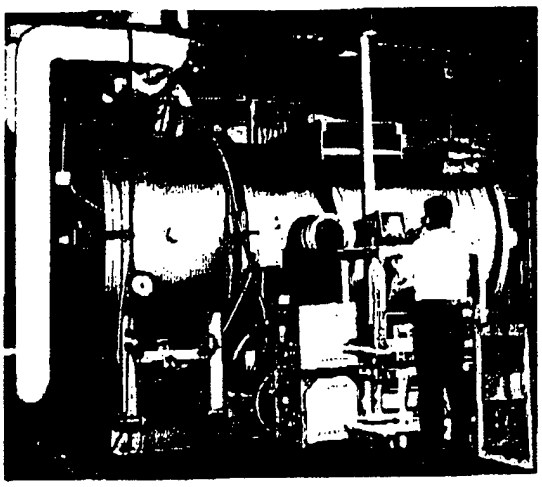

Fig. 3 The T6 vacuum test facility at Busek

Thrust was measured using a NASA Glenn inverted-pendulum type thrust stand nearly identical to that used by Haag et. al.[15] The output voltage from its linear variable differential transformer (LVDT), which is proportional to the thrust, and the inclination of the thrust stand (measured using a capacitive inclinometer), were both measured and recorded using a computer data acquisition system and a strip chart recorder. The experimental procedure used to calibrate the thrust stand prior to and post experiment is identical to that described by Haag.[15] In addition to that procedure, the inclination of the thrust was continuously recorded in an effort to minimize the error associated with changes in the inclination induced by facility thermal effects. The accuracy of the thrust stand is about 1% which is due almost exclusively to zero drift in the LVDT signal conditioning electronics provided that inclination changes are properly accounted for.

The T6 facility is also equipped with plasma probe positioning system, shown schematically in Fig. 4. Several types of probes can be mounted on the end of the tubular probe holder that swings through the plasma beam to probe the beam properties as function of radial distance from the thruster axis and as a function of distance from the thruster exit plane. Two types of probes are typically used: (1) a Faraday cup to determine the ion current density and (2) an emissive probe to measure the plasma potential.

For most of the tests reported herein, the data were recorded using a 12-bit, optically isolated, computer driven data acquisition system. The primary responsibilities of this system were measuring and recording the discharge power, setting and recording the commercial mass flow controllers, measuring the thrust stand's LVDT output and inclination, and recording the vacuum tank pressure along with the cathode and anode internal pressures. To assure validity of the performance data, the commercial mass flow controllers were calibrated on xenon using two independent methods, a constant volume process and a constant pressure process. These methods yield calibration curves that were within 5% of each other for the mass flow rates of interest. Most of the data presented were obtained using a helium leak checked flow system and research grade Xenon having a purity of 99.9995.

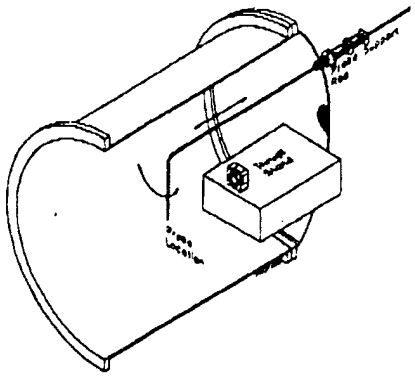

Fig. 4 Mechanical sketch of the T6 facility with its probe positioning system

The BTHT-200 Tandem Hall Thruster was tested with a concurrently developed small hollow cathode. The cathode is shown mounted on the BTHT-200 thruster in Fig. 2. The other thrusters shown in Fig. 2 were tested using a commercial hollow cathode (Ion Tech #HCN-252).

Thruster Design and Performance

There are a number of basic criteria that can be derived and applied to the design and scaling of a Hall thruster. The approach used at Busek and elsewhere[16] is based on the fundamental relationship of the acceleration length (L) to the Ion Larmor Radius (ρ_i) the electron Larmor radius (ρ_e) and ion - neutral mean free path (λ) defined as

$$L > \rho_i = \frac{m_i v_i}{qB} \quad L << \rho_e = \frac{m_e v_e}{qB} \quad L < \lambda \approx \frac{1}{n_n Q_{in}} \qquad [2]$$

where v is the velocity for the electrons and Ions as denoted by the subscripts.

To maintain constants ρ_e, ρ_i, λ and υ

$$n_e \sim n_i = n_o \sim \frac{1}{L} \qquad I_{dis} = n_i \sigma_i q A \sim \left(\frac{1}{L}\right)(L)^2 \sim L$$

$$B \sim \frac{1}{L} \qquad J_{dis} = I_{dis} / A \sim \frac{1}{L} \qquad [3]$$

$$V_{dis} \sim \text{invariant} \Rightarrow E \sim \frac{1}{L} \qquad \text{Power} = V_{dis} I_{dis} \sim L$$

These equations relate the thruster characteristic dimension L to plasma parameters, which are then related to discharge zone geometry thus bridging the relationship of plasma parameters to thruster geometry. Magnetic circuit is then sized using Gauss' and Ampere's law with the final selection (particularly for large size thrusters) based on structural and fabrication considerations.

The sub-kW thrusters in Fig. 2 were designed using the above equations and constructed over a period of the last several years, continually evolving. The circular, 200 W, Tandem Hall Thruster (BTHT-200) is the most developed design, nearly ready for a flight qualification program. The other two thrusters are in a laboratory development stage. However, a larger (4 kW) version of the 600 W design (BHT-HD-600) has successfully completed 4000 hours life test, performed by Primex Aerospace Co., that licensed the technology from Busek. All three designs are patent pending.

The major specifications of the BTHT-200 are shown in Table 1. It has an operating envelope from 50 to 300 Watts. Its nominal thrust is 11.4 mN and the anode I_{sp} approaches 1600 seconds at a discharge voltage of 300 V. It employs a unique magnetic circuit design that can produce and handle the high magnetic flux required in small size Hall thrusters. A single electromagnetic coil is located in tandem (axially consecutive) with two distinct discharge chamber zones. This tandem arrangement overcomes many of the low power thruster design barriers encountered when using the classical scaling (Eq. [2] and [3]).

The 600 W thruster (BHT-HD-600) was designed to operate at high plasma density, which implies a high thrust density. Its performance is listed in Table 2. Consistent with Hall thruster scalling it has higher efficiency and higher specific thruster (thrust per input power) than the lower power BTHT-200. However, life considerations, which have not been adequately explored with this thruster, may force some performance derating, which at this point, surpasses all other known thrusters of comparable size.[17,18,19]

The BHT-RT-150 was constructed to demonstrate that circular shape discharge chamber is not necessary for proper functioning of a Hall thruster. The theory requires that the $\overline{E} \times \overline{B}$ electron drift closes upon itself through a uniform plasma to achieve acceptable performance. This can, in principle, be satisfied with many different shapes. However, these are generally more difficult to construct and achieve proper propellant distribution, matched to the local magnetic field. The racetrack is the simplest shape next to the circular and has several potential advantages over it:

1. It's radial magnetic field gradient $dB_r/dr \approx 0$. This helps to reduce radial electron drift and wall collisions that lead to losses.
2. The racetrack geometry is amenable to thrust vectoring through manipulation of the local magnetic field.
3. In principle any power racetrack thruster can be assembled simply by extending its straight section while keeping the same optimized cross-sectional geometry. This may be especially important in high power (50 to 100 kW) thrusters being considered for the space based solar power station and the Mars mission.

The BHT-RT-150 is the least developed thruster of the three presented. Its typical performance numbers at 150 Watts are T= 7 mN, anode efficiency = 30% and I_{sp} = 1250 sec. However, an AFOSR funded program is under way at Busek to explore some of the issues in a larger multi kW racetrack.

Table 1 BHT-200-X2B Specifications

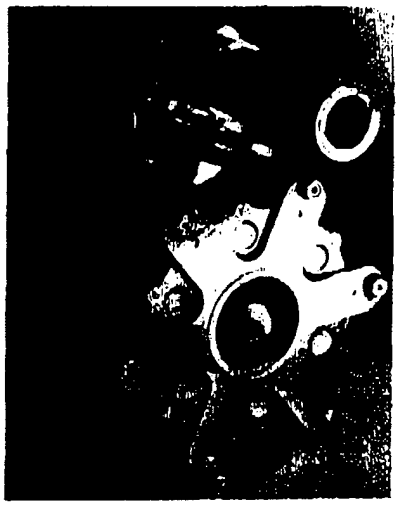

Acceleration Annulus Mid-Diameter	21 mm
Input Power	207 Watts Nominal 100-300 Watts
Discharge Voltage	300 V Nominal 200 - 400 V
Propellant Mass Flow Rate	0.74 mg/sec (Xe) Nominal 0.30 to 1.01 mg/sec (Xe)
Thrust	11.4 mN Nominal 4 to 17 mN
Anode Efficiency	42% Nominal 20 to 45%
Anode Specific Impulse	1570 sec Nominal 1200 - 1600 sec
Thruster Mass	<1 kg
Thruster Dimensions	10.5-cm diameter, 12-cm length

Table 2 BHT-HD-600 Specifications

Acceleration Annulus Mid-Diameter	35 mm
Input Power	600 Watts Nominal 300 - 700 Watts
Discharge Voltage	300 V Nominal 150 - 300 V
Propellant Mass Flow Rate	2.00 mg/sec (Xe) Nominal 1.5 to 2.6 mg/sec (Xe)
Thrust	36 mN Nominal 15 to 45 mN
Anode Efficiency	51% Nominal 35 to 54%
Anode Specific Impulse	1700 sec Nominal 1000 - 1850 sec
Thruster Mass	<2.2 kg
Thruster Dimensions	12-cm H x 12-cm W x 15-cm D

Analysis and Discussion

The plasma behavior downstream of a thruster exit plane has a significant effect on its performance regardless of the thruster size and type. When the ion beam exiting the thruster forms a sharply defined luminescent zone (on the thruster axis of symmetry), its performance increases. We call this zone a jet or a jet mode of operation. It, along with a simple analytical model of the thruster performance, will be discussed in the next section.

The Jet Mode and Two Parameter Performance Model

The ideal versus actual Hall thruster behavior at a constant input power is shown in Fig. 5. Without losses, the thrust (T) should continuously increase with decreasing Isp. Experimental data however indicate a non-ideal thruster behavior where at some Isp the slope of the curve (dT/dI_{sp}) reverses

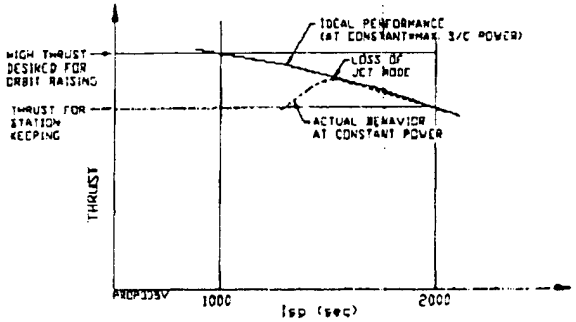

Fig. 5 Idealized versus actual behavior of Hall thrusters at constant input power

The point of reversal generally coincides with the loss of jet mode. To illustrate what is meant by "jet mode," we show in Fig. 6 two photos of the BTHT-200 thruster operating at a constant power but different voltage and mass flow (different Isp). A highly luminescent central jet is clearly visible in the left photo and absent in the right hand photo. Disappearance of the central jet coincides with a steep drop in measured thrust which is identified in Fig. 5 as the "loss of jet mode." Discharge voltage has the strongest influence on the point of transition which is also affected by magnetic field magnitude and distribution, mass flow rate and very importantly the test tank pressure.

In order to understand any physical phenomena it is in general a useful approach to construct the simplest mathematical model that contains enough physics to represent the situation but remains analytically transparent to enhance understanding of the functional relationships. Therefore, we developed a thruster performance model that relies on two easily understandable parameters. One is the flux of cathode electrons that enter the thruster (I_{ee}) to ionize the propellant normalized by the total discharge current ($i = I_{ee}/I_{dis}$) which we illustrate in Fig. 2, and the other parameter is the energy (voltage) loss during the ionization and acceleration process. This loss, labeled ΔV_{itl}, is composed of all voltage drops that do not create thrust and can be written as

$$\Delta V_{itl} = \Delta V_c + \Delta V_A + \Delta V_{pb} + \Delta V_w + N\varepsilon_i ..... \quad [4]$$

where ΔV_C and ΔV_A are the cathode and anode voltage drops, the ΔV_{pb} is the voltage dropped in the plasma bridge between the thruster exit and the cathode, ΔV_w is wall losses, and $N\varepsilon_i$ is some multiple of the propellant ionization potential. (Note that ΔV_A could be either negative or positive depending on the current density, electron thermal speed and area of the anode). Thus the discharge voltage V_{dis} can be written as

$$V_{dis} = V_{acc} + \Delta V_{itl} \quad [5]$$

where V_{acc} is the actual accelerating and hence the useful part of the applied voltage. Typical ΔV_{itl} is 60 to 80 volts which is about the discharge voltage when the applied magnetic field is zero. The magnitude of I_{ee} (or I) is dictated by how many cathode electrons it takes to produce the total discharge current. As shown in Fig. 8, the ionization process is ideally a chain reaction starting with one cathode (primary) electron, which through a collision with a neutral propellant atom produces an extra electron that in turn produces new electrons etc. If we could arrange things in such a way that each electron emerges from an ionizing collision with near zero energy, is then accelerated by the applied voltage to ε_i and collides again to produce the another electron, then one cathode electron could produce N plasma electrons where N is given by

$$N \approx \frac{V_{dis}}{\varepsilon_i} \approx \frac{300}{12} = 25$$

and therefore

$$\left(\frac{I_{ew}}{I_{dis}}\right) = 2^{-25} \approx 0$$

Under these ideal conditions there are no electron losses (inelastic collisions and wall collisions) leading to a high efficiency thruster.

In reality, each cathode electron produces 4 to 8 propellant electrons (2 to 4 ions) because typical experimentally demonstrated value of the primary electron loss parameter (i) is about 0.15 to 0.2.

$$i = \frac{I_{ew}}{I_{dis}} = 0.2 \approx 2^{-N} \Rightarrow N = 2.3$$

Armed with this discussion we can now express the thrust (T), I_{sp} and efficiency (η) in terms of discharge power P_{dis}, and the two loss parameters, i and ΔV_{itl}

$$T = \dot{m}_i < u > \cong \dot{m}_i u_i \cong \left(\frac{2P_{dis}}{I_{sp}}\right)\frac{k_1(1-2i)}{1+\left(\frac{k_1\Delta u_i}{I_{sp}}\right)^2} \quad [6]$$

$$I_{sp} = \frac{T}{\dot{m}_i g_o} \cong \frac{\dot{m}_i u_i}{\dot{m}_i g_o} \cong k_1(1-i)\sqrt{\frac{2q(V_{dis}-\Delta V_{itl})}{m_i}} \quad [7]$$

$$\eta = \frac{\frac{1}{2}\dot{m}_i u_i^2}{P_{dis}} \cong (1-i)\left(1-\frac{\Delta V_{itl}}{V_{dis}}\right) \cong \frac{1-i}{1+\left(\frac{k_1\Delta u_i}{I_{sp}}\right)^2} \quad [8]$$

where $k_1 = \left(\frac{I_{dis}}{\dot{m}_i g_o}\right)\left(\frac{m_i}{q}\right) \cong$ constant ≈ 0.139 for Xe.

$\Delta u_i = \sqrt{\frac{2q\Delta V_{itl}}{m_i}}$ = ion velocity deficit due to ΔV_{itl} loss

and

$P_{dis}=I_{dis}V_{dis}$= applied power, $g_o=9.81 m/sec^2$, $\dot{m}_i$ = total mass flow.

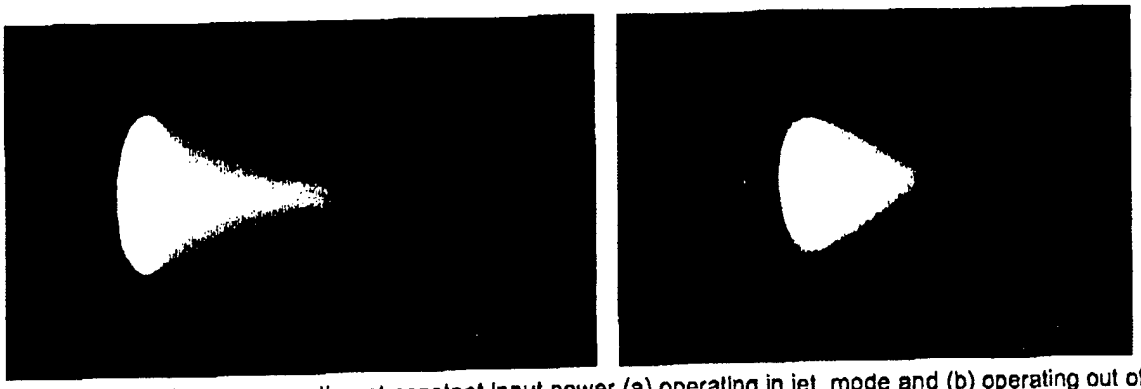

Fig. 8 Typical Hall thruster operation at constant input power (a) operating in jet, mode and (b) operating out of jet mode

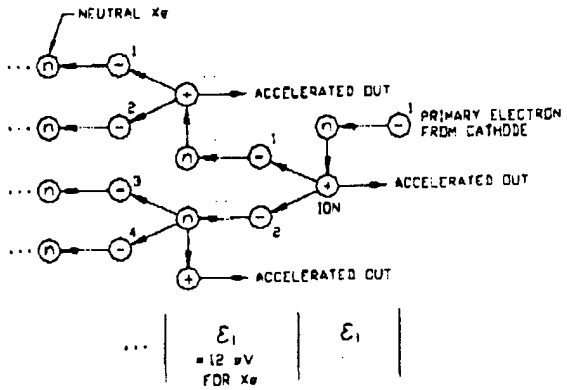

One Cathode electron results in 2 electrons in first collision, in 2^{nd}, 8 in 3^{rd} .....

$$\left(\frac{I_{ec}}{I_{diss}}\right)_{Typical} = 0.15 \approx 2^{-N} \Rightarrow N = 2.74$$

$$N \approx \frac{V_{diss}}{\varepsilon_i} \approx \frac{300}{12} = 25$$

$$\Rightarrow \left(\frac{I_{ec}}{I_{diss}}\right)_{min} = 2^{-25} \approx 0$$

⇒On the average a cathode electron produces 4 to 8 propellant electrons (2 to 4 ions)

Fig. 7 Ionization process in a Hall thruter

The expression for thrust (Eq.[6]), is not a monotonic function of I_{sp}, but has a maxima dependant on ΔV_{ml} and i. The maximum occurs when $k_1\Delta u_i/I_{sp}=1$. It means, that every thruster depending on its losses has an I_{sp} at which it delivers maximum thrust. This maximum thrust specific impulse (I_{sp}^*) can be expressed as

$$I_{sp}^* = k_1\Delta u_i = \frac{2\Delta P}{\Delta T g_o} = \frac{2I_{diss}\Delta V_{ml}}{g_o \dot{m}_i \Delta U_i} \qquad [9]$$

Thus the maximum thrust I_{sp}, is determined by the ratio of power loss (ΔP) and the thrust loss (ΔT), both of which are functions of ΔV_{ml} but not i.

Clearly, minimizing ΔV_{ml} and i leads to the highest thrust and efficiency and small ΔV_{ml} extends I_{sp}^* to a lower value.

Equations [6] and [8] are plotted in Fig. 8. Experimental data from the BHT-HD-600 thruster are superimposed on the theoretical lines for three constant powers of 600, 500 and 400 W. It is seen that our simple two parameter model is in good agreement with data. The assumed values of i and ΔV are 0.15 and 60 volts respectively. Maximum thrust occurs at an Isp ≈ 1200 sec. The only way to further increase thrust is to lower ΔV_{ml} and i, which of course would also improve the thruster efficiency.

As seen from Eq. [8], the efficiency continuously increases with I_{sp} approaching asymptotic value at I_{sp} >4000 sec. Such high I_{sp} requires high V_{diss}. When $\Delta V_{ml}/V_{diss}$<<1, the efficiency becomes $\eta \approx (1-i)$ and hence the asymptote. Therefore maximum efficiency is given by the primary electron loss parameter (i) and the operating voltage limit which in turn is dictated by acceptable thruster life.

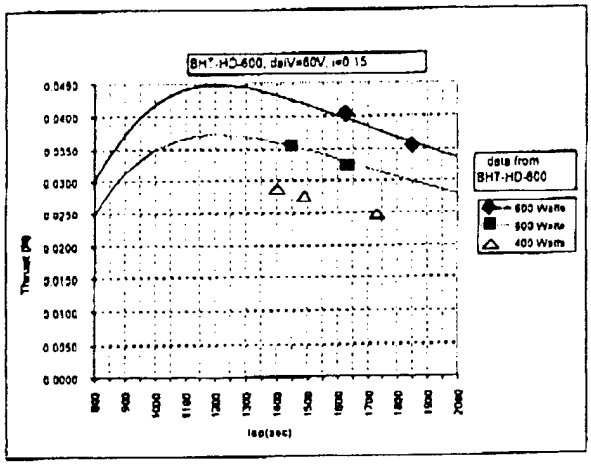

Fig. 8 Thrust and efficiency vs. I_{sp} for an BHT-HD-600

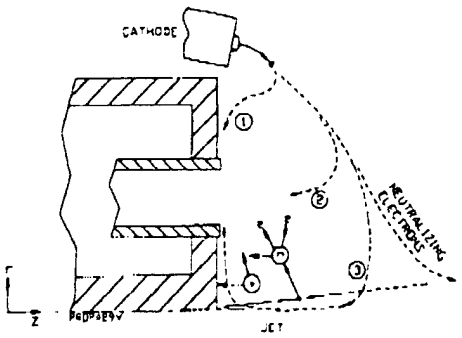

Fig. 9 Preferred electron path from cathode to thruster exit is #3. Path #1 is unlikely because of low local density of neutrals and because the electrons would have to cross strong B field lines as they would follow path #2

It should be noted that for Isp<1200 sec, the predicted drop off in performance is slower than experimentally observed in other Busek thrusters. This is due to two factors. The first is that ΔV_{III} and I are not independent from each other as the model assumes. The second is that when the thruster falls out of jet mode, the performance drops in a step like fashion which probably means step-like increase in ΔV_{III}. We believe as illustrated in Fig. 9, that the jet serves as a low resistance path for electrons (electron highway) from the cathode to the thruster which will be discussed in detail in subsequent sections. When the jet disappears, it abruptly increases ΔV_{III} with corresponding drop in thrust.

The extent to which it may be possible to increase the specific thrust (N/Watt), which is equivalent to lowering I_{sp}*, is illustrated in Fig. 10. The assumed ΔV_{III} is varied from 70 volts to zero. The theoretical limit on ΔV_{III} is the propellant ionization potential (12.13eV for Xe) for which I_{sp}*≈600 sec. Thus no Xe fueled Hall thruster operating at constant power can increase its thrust by lowering I_{sp} (decreasing V_{dis} while increasing mass flow) beyond 600 sec

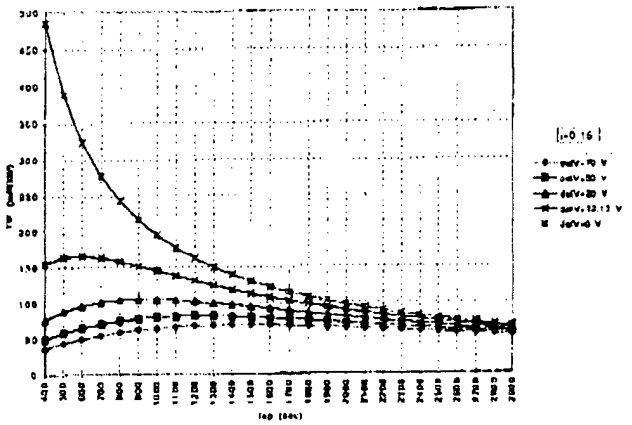

Fig. 10 Specific thrust vs. I_{sp} for various voltage loss ΔV

The Jet Mode - Present Understanding

The jet, visible in the left photograph of Fig. 6 is characterized by a highly luminescent steep angle cone, which has a vertex at the thruster exit plane. At times the vertex is attached to the pole piece but mostly it appears to be detached a few millimeters downstream. When the thruster operates at high efficiency the cone boundaries are sharply delineated by highly luminescent lines (much more luminescent than the cone interior but hard to capture on film) strongly reminiscent of oblique shock in conventional supersonic flows. The lines start at the vertex and extend downstream approximately 3 thruster exit diameters. Beyond that, their intensity fades and become indistinguishable from the cone interior which itself becomes gradually diffused and invisible. The cone included angle is estimated to be about 10° and does not seem to depend strongly on operating conditions.

The thruster transits in and out of the jet mode very abruptly. Once the jet appears the thrust increases by about 10 to 15% in stepwise fashion without any other changes in input conditions. Often the power input drops while the thrust increases. The transition point in and out of the jet mode depends on thruster voltage, magnetic field intensity, mass flow, and vacuum tank pressure (the higher the tank pressure the lower the voltage to transit into the jet mode). This transition in and out the jet mode also has a hysterises. The voltage at which it enters the jet mode is typically higher than the voltage at which it goes out of the jet mode.

The phenomena of the "jet mode" is very complex and not well understood. It is however clear from a large body of experimental data covering all sizes and types of thrusters built by Busek that the "jet mode" operation is a requirement for high performance. Most importantly, it appears that the formation of the jet and associated "oblique shock" is a cause and not the consequence of high performance.

The strongest evidence of this is its dependence on the tank pressure. If the formation of the jet/shock was a function of a phenomena occurring within the thruster only, the thruster performance, i.e., the transition into and out of the jet mode could not depend on the tank pressure. The existence of the shock is an information that cannot be transmitted upstream to the thruster by the ion flow because it is supersonic and also largely collisionless. Communication with upstream is fabricated only by electrons.

From the above description of the jet mode cone it is evident that there are many similarities between it and a typical oblique shock structure in front of a sharply pointed body of revolution in a supersonic flow as sketched in Fig. 11a. If indeed we treat the jet cone as a shock phenomena, then the luminescent lines described above that form a surface of discontinuity in the plasma should be possible to examine using conventional oblique shock analysis. The body of revolution becomes a virtual body required by the condition of axisymetrical flow out of the thruster as shown in Fig. 11b.

However, fundamental conditions for the classical oblique shocks to exist are:

1. The normal velocity to the shock front must be greater than speed of sound.
2. The flow must be collisional with mean free path of the order of the thickness of the shock.

We examine each in turn. The flow of the flow of ions has a sonic speed given by

$$c_i \cong \sqrt{\frac{kT_e}{m_i}}$$

For *Xe* and T_e = 5eV, which on the outside of the thruster is the most one should expect, the ion sonic speed is $c_i \cong$ 2000 m/sec. Using the notation of Fig. 11 the ion velocity normal to the shock is $u_{ni} = u_i \sin(\alpha + \theta)$.

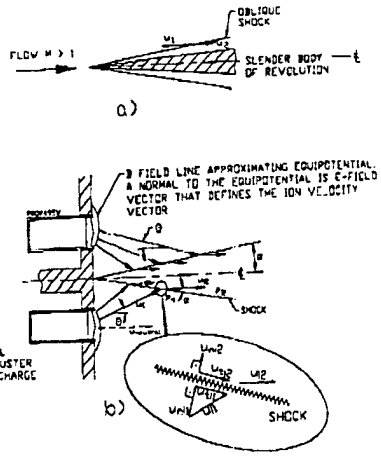

Fig. 11 Similarities between oblique shock in supersonic flow and jet mode shock cone at the exit of a Hall thruster

If we assume $\alpha \approx \theta$, the requirement for the normal component to be supersonic can be written as

$$u_n = \sqrt{\frac{2q(V_{dis} - \Delta V_{ni})}{m_i}} \sin 2\theta > c_i$$

To satisfy this condition the discharge voltage must be

$$V_{dis} > \Delta V_{ni} + \frac{c_i^2 m_i}{2q \sin^2 2\theta} \qquad [10]$$

For *Xe*, ΔV_{ni} = 80V, θ = 10° and T_e = 5 eV, the discharge voltage is about 100V. For T_e = 50 eV it is $V_{dis} \cong$ 290V. Thus ion velocity normal to the shock exceeding sonic velocity can be achieved well within the operating range of the thruster and the condition in item 1 above is satisfied.

It is also important to realize that Eq. [10] can be written as

$$c_i < \frac{2q(V_{dis} - \Delta V_{ni})}{k} \sin 2\theta \qquad [11]$$

Therefore the existence of an oblique shock puts an upper bound on the electron temperature and Eq. [11] can be used to estimate T_e. (The angle θ can be visually observed, V_{dis} is measured, and ΔV_{ttl} can be safely assumed to be between 60 to 80V). If we say that the shock appears at V_{dis} = 200 V (and assume that ΔV_{ttl} = 80V and θ = 10°) then T_e < 28 eV.

To examine the condition in item 2 above, we estimate the ion-neutral mean free path to be

$$\lambda \sim \frac{1}{n_n Q_{in}} = \frac{kT}{pQ} \cong 5m \text{ for } p \approx 10^{-4} Torr$$

Therefore it follows that the luminous line discontinuity we see cannot be a conventional shock even if the λ is two orders lower than the above estimate (the inflow of the ions toward the center could explain one order of magnitude). The only remaining possibility is that the discontinuity is a shock but a collisionless shock created when supersonic ions interact with electric or magnetic fields. The most well known example is the bow shock around our planet created by the Earth magnetic field interacting with the incoming charged particle from space. In our situation the shock can form only if the plasma (ions) "collide" with decelerating potential (step up in voltage) or if it runs into strong magnetic field lines. Chen[20] analyzed a similar situation and we can follow his approach.

We assume that the temperature of the heavy species on both sides of the shock is negligible ($\cong$0). Conservation of ion energy then leads to

$$\frac{mu_1^2}{2} = \frac{mu_2^2}{2} + q\phi$$

and conservation of ion mass requires that

$$u_{1n} n_1 = u_{2n} n_2 \text{ and } u_{1t} = u_{2t}$$

where ϕ is the deceleration potential, subscripts 1 and 2 refer to quantities upstream and downstream of the shock, respectively. Combining the equations give ion density ratio across the shock

$$\frac{n_2}{n_1} = \left[1 - \frac{2q\phi}{mu_1^2 \sin^2\sigma}\right]^{-1/2} \qquad [12]$$

where σ is the angle between u_1 and the shock front.

Poisson's equation downstream of the shock is

$$\frac{d^2\phi}{dx^2} = \frac{q}{\varepsilon_0}(n_e - n_i) \qquad [13]$$

where n_i is our ion density (n_2) downstream of the shock. The electron density can be expressed by Boltzman equation

$$\frac{n_e}{n_1} = \exp\left(\frac{q\phi}{kT_e}\right) \qquad [14]$$

Combining Eqs. [12], [13], and [14] yields

$$\frac{d^2\phi}{dx^2} = \frac{qn_1}{\varepsilon_0}\left[\exp\left(\frac{q\phi}{kT_e}\right) - \left(1 - \frac{2q\phi}{mu_1^2 \sin^2\sigma}\right)^{-1/2}\right] \qquad [15]$$

Charge neutrality requires that the term in the bracket is zero. This leads to

$$0 = \exp(\bar{\phi}) - \left[\frac{1}{1 - \frac{2\bar{\phi}}{M_1^2 \sin^2\sigma}}\right]^{1/2} \qquad [16]$$

where

$$\bar{\phi} = \frac{q\phi}{mc_1^2}$$

$$M_1 = \frac{u_1}{c_1} = \frac{u_1}{(kT_e/m_i)^{1/2}}$$

For the second term in Eq. [16] to be non-imaginary and not go to infinity leads to

$$M_1^2 \sin^2\sigma > 2\bar{\phi}$$

The upstream ion Mach number M_1 has a normal component to the shock M_{1n} given by $M_1 \sin\sigma$ and therefore

$$M_{n1}^2 > 2\phi \qquad [17]$$

For the shock to exist the normal Mach number must be $M_{n1}>1$ and therefore the $\bar{\phi} \geq 0.5$. This value and T_e = 5eV yields ϕ = 2.5V, which, given typical error bars in plasma potential measurements, is almost an undetectable potential rise across the shock. More importantly, no ions could be reflected back toward the thruster by this potential and therefore, could not cause sputtering of the thruster face.

Equation [15] is essentially that of a plasma sheath which is the way our shock can be viewed. Chen[20] shows that solution for ϕ can be oscillatory (single ion acoustic shock wave propagating through plasma is called soliton) and that there is a range of Mach numbers for which it can exist. This range is

$$1 < M_{n1} < 1.6$$

Eq. [17] then yields ϕ_{max} = 1.28 giving the maximum potential step ϕ_{max} to be

$$\phi_{shock} = 1.28\left(\frac{kT_e}{q}\right) = 6.4 Volts \text{ for } T_e = 5eV$$

So far we may have explained what the shock is, i.e., stationary plasma sheath but have not explained how it effects the thruster. This is addressed in the next subsection.

Effect of Ion Acoustic Shock on Plasma Conductivity and Thruster Performance

If our assumption that the ion temperature on either side of the shock is negligible the issue becomes where does the energy go. The most likely answer is into excitation and ionization of neutrals within the cone of the shock -- the jet. From Eq. [12] it is clear that $n_1/n_2 < 1$ and therefore the ion density within the shock cone is higher than outside of it. Charge neutrality then requires n_e to be higher within the cone. The electrons are also trapped by magnetic lines and more importantly by the unfavorable potential step ϕ. Electron/neutral collisions excite (causing luminescence) or ionize neutrals whose density is a function of tank pressure only. The electrical conductivity ($\sigma \sim n_e$) within the shock cone or a jet is then much higher than outside of it and the jet acts as a "highway" for electrons (path #3 in Fig. 9) on their way to the thruster. (As will be shown in the next section presenting experimental data, the jet plasma potential is positive and is a function of tank pressure which supports the above statement). This low voltage drop path then increases the useful part of the discharge voltage (see Eq. [4]) leading to higher efficiency and higher thrust. A contributing factor to the step increase in thrust may also be the production of ions within the shock cone/jet which are then accelerated downstream by the favorable axial electric field. This is consistent with the shock dependence and thrust dependence on tank pressure -- increasing neutral density feeds neutrals by diffusion into the cone which are then expelled as ions (acting as electrostatic ion pump).

Jet Mapping - Experimental Results

Using the 200 W Hall thruster an experiment was conducted to measure the plasma potential and ion current density as a function of axial and radial distance from the thruster. The photograph in Fig. 12 shows this thruster and its plume being seemed by a Faraday probe. Some of the results are shown in Fig. 13 and 14. Presented on Fig. 13 is a color contour map showing the variation of the plasma potential in the region downstream of the thruster. The thruster was operated at 0.72 mg/sec Xe thruster flow, a discharge current and voltage of 0.67 A and 300 V. The tank pressure was 2 x 10^{-5} Torr. Under these operating conditions, the jet and the ion acoustic shock lines are clearly visible, yet we did not detect sharp voltage discontinuity of the order of a few volts that is predicted by the ion acoustic shock analysis in the previous section. It should be noted however that data were obtained at discrete axial positions (i.e. 1-cm, 2-cm, 3-cm ...) and therefore some of the potential variations is an artifact of the curve fitting routine used to generate the figure.

Fig. 12 BHT-200-X2 200 Watt Hall thruster operating in the plume mode. Also shown is the emissive and Faraday probes

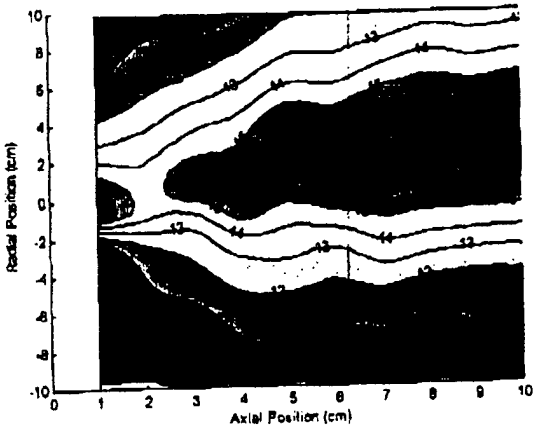

Fig. 13 Typical plasma potential color contour map

The Faraday probe ion beam data were synthesized into Fig. 14 which shows a scaled cross sectional view of the thruster, the ion current density contour map, and probable boundaries for the ion beam. Superimposed on the data is the visually observed ion acoustic shock. To determine the ion beam boundaries, the deposition pattern on the exit insulator was examined to indicate the probable acceleration zone location. Using this information, lines were drawn to show the convergence of the ion beam at a axial position of 3.5-cm. From this point downstream, the ion beam continues at the same low divergence angle as shown by the dashed lines downstream of 3.5-cm. Extending the dashed lines to 11-cm yields a beam radius of about 2.5-cm,

confirming the results of a Faraday probe scan at that location which shows a beam diameter of 5-cm. As explained in the previous section, the ion acoustic shock decelerates the ion velocity component normal (orthogonal) to the shock and turns the flow downstream of the shock to be more parallel to the thruster axis. Because the ions near the inner beam boundary have trajectories with small normal (to the shock) velocity component, their trajectory is not significantly changed. The ions near the outer beam boundary, however, undergo more significant redirection and as a result the beam divergence beyond the 3.5-cm focal point is low. It should be noted that these results are preliminary and subject to further study.

Conclusions

Three different sub-kilowatt thrusters were constructed and tested. Their performance is among the highest for their size and matching or exceeding the published data of comparable thrusters made by others.[17,18,19] Simple analytical model was developed that correctly predicts Hall thruster performance, given two loss parameters (i and ΔV_{ii}). Attempt was made to explain the nature of the highly luminescent central jet and why its presence or absence, which primarily voltage and test tank pressure dependant, has such a strong effect on the thruster performance. Based on visual observations and modeling the cone boundaries, were tentatively identified as an ion acoustic shock. The included angle of the oblique cone shock is predicted to be a function of the plasma electron temperature (T_e) and measurement of the angle can be used to predict T_e. The plasma inside the cone is highly conductive and acts as a highway for electrons. This lowers voltage loses in the plasma bridge between the cathode and the thruster, improving its performance. Ionization of neutrals inside the cone which are subsequently accelerated downstream by a favorable voltage gradient could also contribute to the increased thruster performance when the jet cone appears.

Acknowledgments

The authors would like to thank Dr. Ron Spores and Dr. Keith McFall, the AFRL technical program monitors of the 200 W (BTHT-200) thruster development contract.

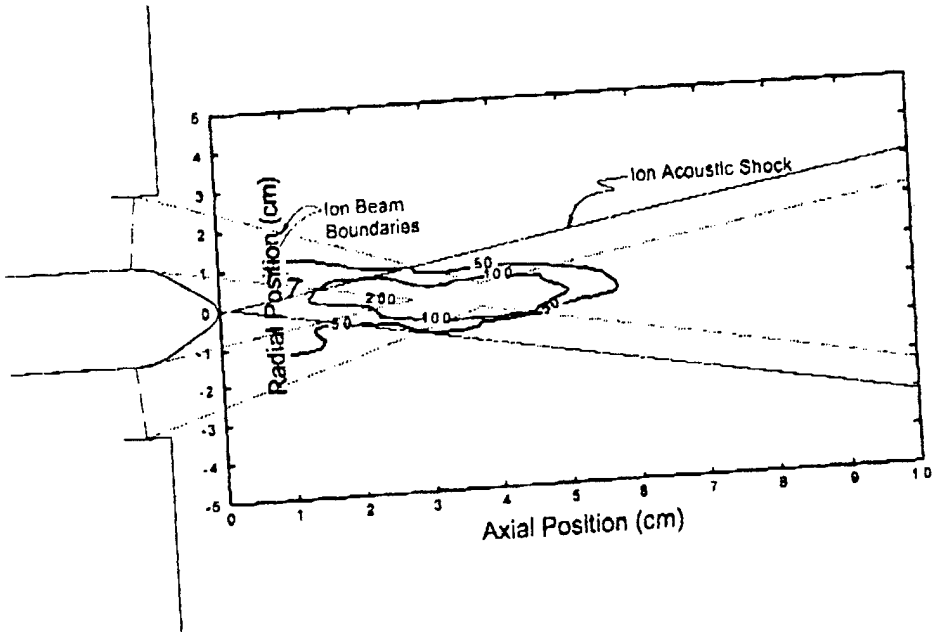

Fig. 14 Conceptual mechanism for the "jet" formation

References

1. Rosa, R.J., Magnetohydrodynamic Energy Conversion, McGraw-Hill, New York, 1968.
2. Sutton, G.W. and Sherman, A., Engineering Magnetohydrodynamics, McGraw-Hill Book Co., New York, 1965.
3. 33rd Symposium on Engineering Aspects of MHD, Tullahoma, June 1995.
4. Pierson, E.S, Branover, H., Fabris, G. and Reed, C.B., "Solar-Powered Liquid-Metal MHD Power Systems," ASME paper 79-WA/Sol-22, 1979.
5. Brogan, T.R., "The 20 MW LORHO MHD Accelerator for Wind Tunnel Drive-Design, Construction and Critique," 30th Plasmadynamics and Laser Conference, Norfolk, VA June 1999.
6. Rosa, R. "Magnetohydrodynamics Applied to Aerospace and Deep Space Propulsion," AIAA/ASME 3rd Joint Thermophysics, Fluids, Plasma and Heat Transfer Conference, Paper No. AIAA-82-1212, St. Louis, June 1982.
7. Cole, J., Campbell, J. and Robertson, a., "Rocket-Induced Magnetohydrodynamic Ejector - A Single-Stage-to-Orbit Advanced Propulsion Concept," AIAA-95-4079, AIAA 1995 Space Programs and Technologies Conference, Huntsville, AL Sept. 1995.
8. Swallom, D., Sadovnik, I., Gibbs, J., Gurol, H., Ngnuen, L. and Van den Bergh,. H., "Magnetohydrodynamic Submarine Propulsion Systems," *Naval Engineers Journals*, Vo. 103, no. 3, May 1991, pp 141-157.
9. Lineberry, J., "Assessment of Hypersonic MHD Concepts," AIAA-97-2393, AIAA Plasmadynamics and Laser Conference, Atlanta, GA, June 1997.
10. Hruby, V.J., "Wake Non-Uniformity In MHD Plasma," AIAA 21st Aerospace Sciences Meeting, Paper No. 83-0398, Reno, January 1983.
11. Garkusha, V., et. al, "Modern Status of Hall Thruster Development in Russia," AIAA-99-2157, AIAA 25th Joint Propulsion Conference and Exhibit, June 1999.
12. Saccoccia, G. "European Electric Propulsion Activities and Programes," AIAA-99-2158, AIAA 25th Joint Propulsion Conference and Exhibit, June 1999.
13. Dunning, J. and Sankovic, J., "An Overview of the NASA Electric Propulsion Program," AIAA-99-2161, AIAA 25th Joint Propulsion Conference and Exhibit, June 1999.
14. Cohen, R., Spores, R. and Birkan, M., "Overview of Air Force Program in Electric Propulsion," AIAA-99-2162, AIAA 25th Joint Propulsion Conference and Exhibit, June 1999.
15. Haag, T.M. and Osborn, M., "RHETT/EPDM Performance Characterization," IEPC-97-107, 25th IEPC, Cleveland, OH August 1997.
16. Khayms, V. and Martinez-Sanchez, M., "Design of a Miniaturized Hall Thruster for Microsatellites," 32nd AIAA/ASME/SAE/ASEE Joint Propulsion Conference, Lake Buena Vista, FL, July 1996.
17. Jacobson, D.T., and Jankovsky, R.S., "Test Results of a 200 W Class Hall Thruster," AIAA 98-3792, 34th Joint Propulsion Conference, Cleveland, OH, July 1998
18. Manzella, D. and Oleson, S., "Evaluation of Low Power Hall Thruster Propulsion," AIAA 96-2736, 32nd Joint Propulsion Conference, Lake Buena Vista, FL 1996.
19. Ashkenazy, J., Raitses, Y., and Applebaum, G., "Low Power Hall Thrusters for Small Satellites," Proceeding From Israel Annual Conference on Aerospace Science, Feb 1997, pp. 424-434.
20. F.F. Chen, Introduction to Plasma Physics, Plenum Press, New York